

Late infection by Inclusion body hepatitis (IBH) virus in broiler chickens with special attention to its effect on immune organ indices, blood biochemistry and histopathological changes in some organs

Shaimaa Farag^{1*}, Ahmed E. Saad¹, Ebrahim M. Elboraey¹, Kamel A. Zayan¹, Ahmed M. Helal²

¹Department of Avian and Rabbit Diseases, Faculty of Veterinary Medicine, Benha University, Egypt.

²Central Laboratory for Evaluation of Veterinary Biologics, Abbassia, Agriculture Research Centre (ARC), Egypt.

ARTICLE INFO

Received: 01 October 2024

Accepted: 27 October 2024

*Correspondence:

Corresponding author: Shaimaa Farag
E-mail address: Shaimaafarag17@gmail.com

Keywords:

IBH, Broiler, Immune organ indices,
Blood chemistry.

ABSTRACT

In this study, we utilized clinical chemistry, immune organ indices, and histopathological evaluations to investigate the impact of late Inclusion Body Hepatitis (IBH) virus infection on broiler chicks reared under identical field conditions with a standardized vaccination protocol. We designed our experiment as follows: 120 one-day-old broiler chicks were divided into four groups. Groups A and B received identical vaccination programs, while Groups C and D did not receive vaccinations. IBH virus infection was conducted on Groups A and C at 24 days of age. We evaluated various parameters including clinical signs, mortality rates, and histopathological changes in the liver, trachea, kidney, and bursa, alongside IBH virus shedding. Plasma samples were collected at each time point from chicks in each group, and the following clinical chemistry analytes were assessed: aspartate aminotransferase (AST), total protein, albumin, uric acid, and lipase. Our findings indicate that IBH virus infection negatively impacted organ health and blood parameters.

Introduction

Fowl aviadenoviruses (FAdVs) belong to the family Adenoviridae, genus Aviadenovirus, being further classified into five species (A–E) (Harrach *et al.*, 2012). Throughout the years, various papers revealed the involvement of certain species in specific diseases. Therefore, adenoviral gizzard erosions (AGEs) are caused by certain strains of FAdV belonging to species A, hepatitis-hydropericardium syndrome (HBS) is caused by some strains of species C, and inclusion body hepatitis (IBH) is caused by some strains of species D and E (Hess, 2013).

Reports of IBH outbreaks in many regions in recent years highlight the disease's global spread (Ojkc *et al.*, 2008; Marek *et al.*, 2010; Lim *et al.*, 2011; Steer *et al.*, 2011; Maartens *et al.*, 2014). In fact, IBH outbreaks cause significant economic losses due to decreased productivity and higher flock mortality. Additional subclinical illness potential was shown by field investigations (De Herdt *et al.*, 2013). On the other hand, multiple *in vivo* investigations indicated various consequences of the induced IBH in chickens (Hess, 2013).

There is a need for new disease monitoring tools to enhance our understanding of the underlying mechanisms in the pathogenesis of IBH. This need may be met by clinical chemistry analytes that are relevant to the health and function of organs that are directly impacted by FAdVs. These analytes can also be utilized as biomarkers to evaluate which pathogens are present.

Clinical chemistry has been extensively employed to monitor the health of individuals in mammals. In contrast, fewer research has been conducted in poultry to provide insight into several diseases, including IBH, from which only some preliminary data has been provided. (Köhler and Hromatka-Vasicek, 1974; Henry *et al.*, 1978; Sandhu *et al.*, 1998; Matos *et al.*, 2016).

Therefore, the objective of the present study was to study the Effect of late Adenovirus infection after the application of a normal routine vaccination programme in commercial broiler chicken on blood chemistry,

immune organs and pathological changes.

Materials and methods

Ethical approval

The experiment was performed in agreement with the recommendations of the animal welfare committee after approval of the protocols, Research Ethics Board, Faculty of Veterinary Medicine, Benha University, Egypt (No.: BUFVTM 05-04-23).

Viruses and vaccines

The FadV-8a reference strain (KT781516) was kindly provided by Radwan *et al.* (2019). Infection occurred by inoculating chickens intramuscularly with 0.2 ml of 107 TCID₅₀ FAdV-8a strain (Chen *et al.*, 2020).

The following commercially available vaccines were used in accordance with the manufacturers' guidelines, IBD vector vaccine (VAXX-ITEK® HVT+IBD) Boehringer Ingelheim, Germany. Live IBD vaccine based on strain (228E) Intervet International B.V Boymeer, Holland, IB live variant Nobilis® IB 4/91 and classical vaccines Nobilis® H120 IB MSD Animal Health, Egypt.

Birds

Commercial broiler chicks were provided from Cairo-3A Company, Egypt. Different groups of chicks were raised on deep litter system each group in separate isolated chamber. Water and feed were provided *ad libitum*.

Experimental design

A total of 120 one-day old broiler chicks were divided into four

Table 1. Experimental Design.

Groups	1 day old	8 days old	12 days old	14 days old	24 days old
GP A (VI)	IBD vector vaccine	IB classical vaccine	IBD live vaccine	IB live vaccine	IBH inf.
GP B (VNI)	IBD vector vaccine	IB classical vaccine	IBD live vaccine	IB live vaccine	-
GP C (NVI, Positive control)	-	-	-	-	IBH inf.
GP D (NVNI, Negative control)	-	-	-	-	-

VI: Vaccinated Infected; VNI: Vaccinated Not Infected; NVI: Not Vaccinated Infected; NVNI: Not Vaccinated Not Infected.

groups (30 chick/group) in four separate chambers in Laboratory Animal Research Unit at the Faculty of Veterinary Medicine, Benha University, Egypt. The experimental design is summarized in Table 1.

Random cloacal swabs were taken on the first day of age from all groups to check absence of IBH virus. Three cloacal swabs were collected on the 5th, 7th, and 9th DPI for IBH viral shedding assessment by Real-time PCR. Three birds were selected for gross lesions and histopathology of Liver, bursae, kidney and trachea on the 5th, and 7th DPI.

Immune organs indices (bursa-thymus and spleen) were calculated according to the formula: (immune organ weight x 100)/body weight (Tanimura *et al.*, 1995).

Blood samples were collected on the 3rd, 5th, 7th and 9th DPI for blood biochemistry parameters.

Pathology

The collected Liver, bursae, kidney and trachea of the different groups were preserved and fixed in 10% buffered formalin for 24 hours. The specimens for histopathology were dehydrated in several grades of alcohol, embedded in paraffin, and sectioned at 4 microns thickness, then stained by H&E stain according to Bancroft and Gamble (2008).

Real-Time PCR Analysis for IBH virus shedding

DNA extraction from samples was performed using the QIAamp DNA Mini kit (Qiagen, Germany, GmbH) with modifications from the manufacturer's recommendations.

Primers used were supplied from Metabion (Germany) and are of L1 loop of the hexon gene: The nucleotide sequences of the primers were as follows: adeno-F- 5'-ACATGGGAGCGACCTACTTCGACA-3' and adeno-R- 5'-TCGGCGAGCATGTACTGGTAAC-3'.

Primers were utilized in a 25 µl reaction containing 12.5 µl of 2x QuantiTect SYBR Green PCR Master Mix (Qiagen, GmbH, Germany), 0.5 µl of each primer of 20 pmol concentration, 8.5 µl of water, and 3 µl of DNA template.

The reaction was performed in a MX3005P real-time PCR machine (Agilent, CA, USA). The following conditions were used: 5 min. at 94°C for primary denaturation, 40 cycles for amplification that included 3 steps of secondary denaturation at 94°C for 30 sec., annealing at 60°C for 40 sec., extension at 72°C for 45 sec., Final step dissociation curve for 1 cycle included 3 steps of secondary denaturation at 94°C for 1 min., annealing at 60°C for 1 min., final denaturation at 94°C for 1 min. (Adel *et al.*, 2021).

Clinical chemistry

Blood was collected from the jugular vein of birds into heparin tubes on the 3rd, 5th, 7th and 9th DPI. Tubes were centrifuged and plasma was separated then stored at -20°C till work. The following Five clinical chemistry analytes were investigated aspartate aminotransferase (AST), total protein, albumin, uric acid and lipase (Matos *et al.*, 2016).

Statistical analysis

Statistical analysis was conducted with the Statistical Package for Social Science (SPSS Inc. Released 2021) to determine if variables differed

among groups. Comparison among means was conducted by one-way ANOVA.

Results

Clinical signs and mortalities

It was observed that birds of groups A and C were huddled together and showed depression between the 3rd and 9th DPI. The birds suffered profuse diarrhea. In contrast, groups B and D showed no signs of illness. During the investigation, no mortalities were reported.

Gross pathology

On necropsy liver of infected groups showed pinpoint hemorrhages giving mosaic appearance, in other cases there was subcapsular hemorrhage. In some cases, we recorded hydropericardium (Fig. 1).

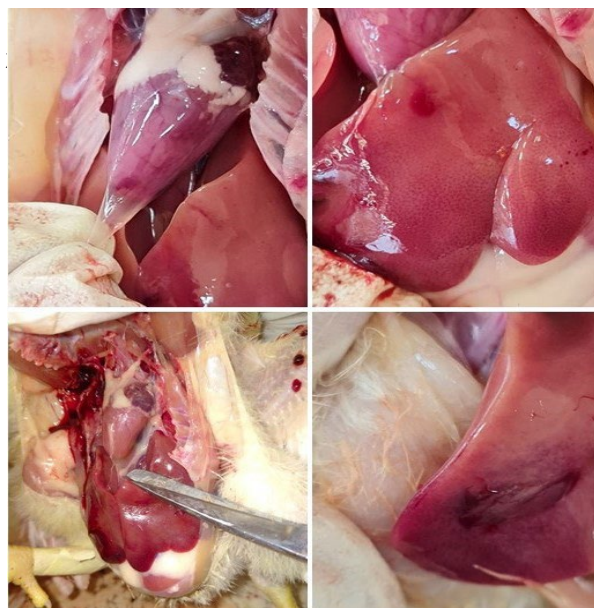


Fig. 1. Postmortem lesions. Left-sided pics. reflect hydropericardium lesions from infected groups, right-sided showing a marble-shaped appearance of infected livers and subcapsular hemorrhages.

IBH shedding

Group A, comprising vaccinated and infected birds, demonstrated detectable virus shedding on the 5th, 7th and 9th days post-infection (DPI). The highest viral shedding was detected on the 5th DPI. Conversely, Groups B and D exhibited no evidence of virus shedding throughout the sampling period. Group C displayed detectable virus shedding akin to Group A (Table 2).

Blood biochemistry

There is a significant difference between groups for all parameters ($p < 0.05$). Infected groups (A and C) showed higher levels when compared to (B and D). The Highest level of Lipase was on the 3rd DPI, for AST was on the 5th and 7th DPI, for total protein and albumin was the 5th DPI, and

uric acids was on the 5th and 9th DPI (Fig. 2).

Table 2. Cloacal shedding of IBH virus in different groups.

Groups	Cloacal swabs		
	5 th DPI	7 th DPI	9 th DPI
A	14.21 ^a ±1.69	12.21 ^a ±1.20	20.78 ^a ±1.54
B	nd	nd	nd
C	17.57 ^b ±1.01	13.49 ^b ±1.77	22.68 ^b ±2.15
D	nd	nd	nd

Data are presented as mean of number of CT± St. deviation. Values with different letters are significantly different (p<0.05) in the interaction between groups and time. n.d.= not detected.

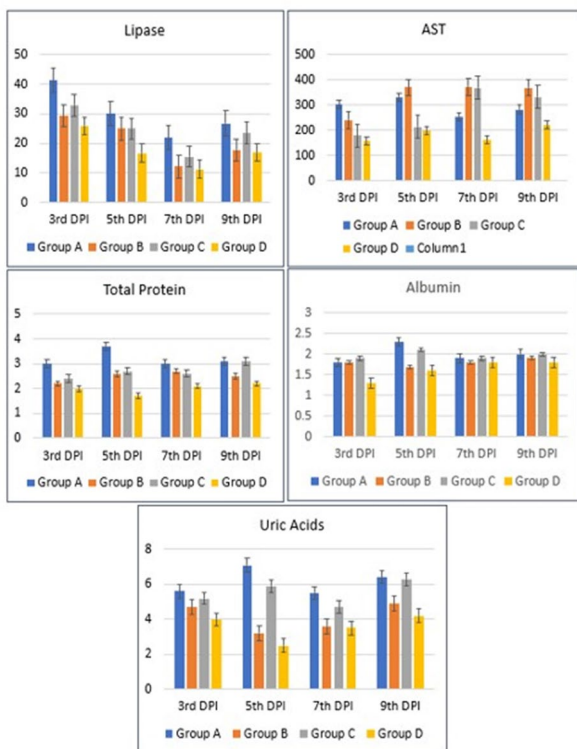


Fig. 2. Graphical illustration of statistical analysis of Blood biochemistry for groups. Group A “vaccinated infected”, Group B “vaccinated not infected”, Group C (positive control) “non vaccinated infected”, Group D (negative control) “non vaccinated non infected”.

Immune Organs’ indices

Considering the bursal index, groups A, B, and C recorded a significant decrease(p<0.05) in the bursal index when compared to group D. Group A represents the most decrease between groups on both the 5th and 7th DPI. The Thymus index shows the same criteria as the bursal index on the 5th DPI while at the 7th DPI groups C and D had no significant difference. For splenic index groups A, B, and C showed a significant increase(p<0.05) of their indices in comparison to Group D (Fig. 3).

Histopathological findings

Liver

Microscopic examination of liver tissues from the negative control group exhibited typical histological features consistent with a healthy avian liver. Hepatocytes displayed a regular polygonal shape with distinct cell borders and centrally located round nuclei. The hepatic lobular architecture was well-preserved, with hepatic cords radiating from the central vein and arranged in a radial pattern. Sinusoids appeared patent, with Kupffer cells sparsely distributed along their endothelial lining. Meanwhile, the liver tissues from the vaccinated not infected group demonstrated minimal histological changes compared to the negative control group. Hepatocytes maintained their typical morphology, with no evidence of vacuolar degeneration or inflammatory cell infiltration.

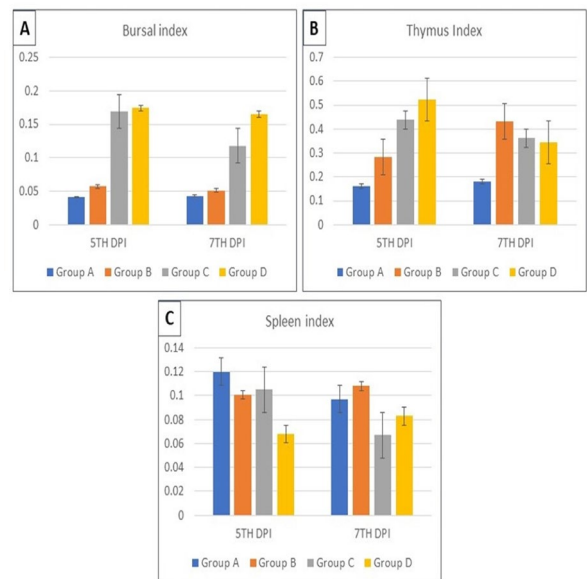


Fig. 3. Statistical analysis of Immune organ indices. A) Bursal index. B) Thymus index. C) Spleen index. Group A “vaccinated infected”, Group B “vaccinated not infected”, Group C (positive control) “non vaccinated infected”, Group D (negative control) “non vaccinated non infected”.

The hepatic lobular architecture remained intact, and sinusoids appeared patent with no signs of congestion or dilation. Following IBH infection, histopathological analysis of liver tissues from the positive control group revealed notable alterations indicative of viral pathogenesis. Hepatocytes displayed varying degrees of vacuolar degeneration and cytoplasmic changes, suggesting cellular injury. Additionally, mild inflammatory cell aggregation, predominantly lymphocytes, was observed in the hepatic tissue on the 5th DPI. Sinusoidal dilatation and congestion were also noted, reflecting impaired liver function and blood flow disruption. While on the 7th DPI, the inflammatory cell aggregates were massive and replaced large areas of the hepatic tissue. The portal areas showed marked congestion and dilatation of the portal vein with hyperplasia of the biliary epithelium in association with formation of newly formed bile ductules. Additionally, the lumen of the bile duct was expanded with eosinophilic debris. Occasionally, the portal areas were expanded by moderate numbers of leukocytes, mainly lymphocytes and variable amounts of fibrous tissue proliferation. Liver tissues from vaccinated infected group exhibited a mixed histopathological profile reflecting both the protective effects of vaccination and the pathological consequences of viral infection (Fig. 4).

Bursa of Fabricius

Histopathological examination of the bursa of Fabricius tissues from the negative control group revealed characteristic features consistent with a healthy avian immune organ. Lymphoid follicles within the bursal tissue exhibited well-defined architecture, with prominent germinal centers surrounded by densely packed lymphocytes. The follicular epithelium appeared intact, forming distinct borders around the follicular structures.

Interfollicular spaces were observed to be minimal, with sparse connective tissue present. Meanwhile, histopathological examination of the bursa of Fabricius tissues from the vaccinated not infected group on the 5th DPI demonstrated features of Lymphoid follicles exhibited hypertrophy, with enlarged germinal centers and increased numbers of actively proliferating lymphocytes. While on the 7th DPI, the follicular epithelium appeared intact, with minimal tissue architecture disruption. Notably, the interfollicular spaces showed mild widening, suggesting early immune activation.

In the infected group (positive control), the bursa of Fabricius tissues on the 5th DPI revealed marked alterations indicative of pathological changes following viral infection. Notably, lymphoid depletion was ob-

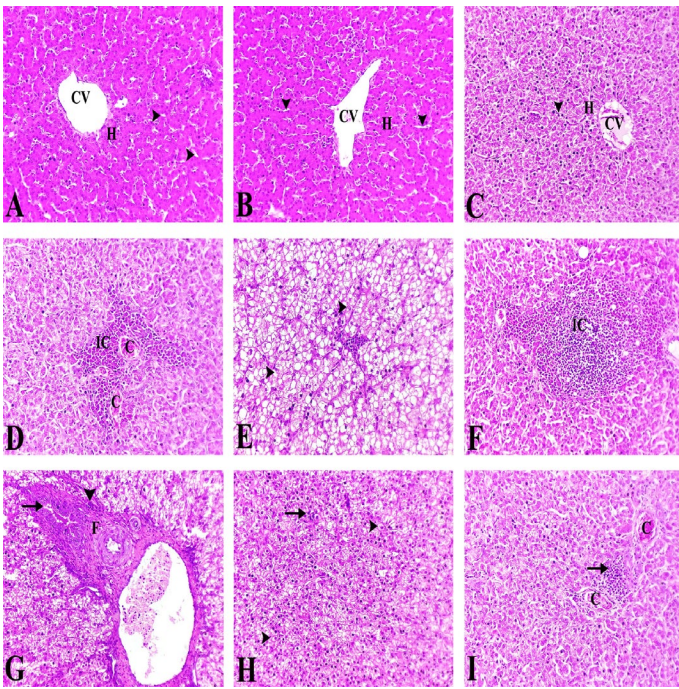


Fig. 4. Histopathological changes of liver post infection. (A) Negative Control group, showing normal histological appearance of central vein (CV), radiating hepatic cords, hepatocytes (H) and patent sinusoids (arrowhead). (B) Vaccinated group on the 5th DPI, showing typical hepatocytes (H) morphology with patent sinusoids (arrowhead). (C) Vaccinated group on the 7th DPI, showing typical hepatocytes (H) morphology with patent sinusoids (arrowhead). (D & E) IBH infected group on the 5th DPI, mild inflammatory cell (IC) aggregation, predominantly lymphocytes in the hepatic parenchyma with congested (C) sinusoid, (D) marked diffuse vacuolar degeneration (arrowhead) of hepatocytes. (F & G) IBH infected group on the 7th DPI, marked inflammatory cell (IC) aggregates replaced large areas of the hepatic tissue, (D) the portal areas expanded by moderate numbers of leukocytes mainly lymphocytes (arrowhead) and variable amounts of fibrous (F) tissue proliferation in association with biliary epithelium hyperplasia (arrow). (H) Vaccinated infected group on the 5th DPI, intact hepatocytes with activation of Von Kupffer cell (arrow), (F) focal areas of vacuolar degeneration (arrowhead) and mild inflammatory cell infiltration (arrow). (I) Vaccinated infected group on the 7th DPI, occasionally mild histopathological lesion were detected in the form of hepatic vascular dilatation and congestion (C) with perivascular inflammation (arrow).

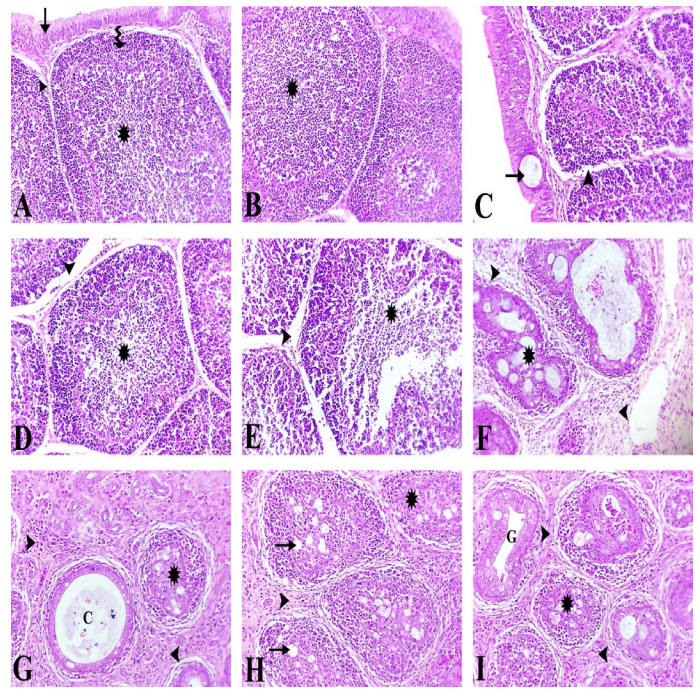


Fig. 5. Histopathological changes of Bursa. (A) Negative Control group, showing normal histological appearance of bursa with intact follicular surface epithelium (arrow) and compact lymphoid follicles with prominent germinal centers (star) surrounded by densely packed lymphocytes (zigzag arrow) with sparse interfollicular spaces (arrowhead). (B) Group B, Vaccinated not infected group, on the 5th DPI showing follicular hypertrophy with enlarged germinal centers (star) and increased numbers of actively proliferating lymphocytes. (C) Group B, Vaccinated group, on the 7th DPI showing mild widening of the interfollicular spaces (arrowhead) and minimal tissue architecture disruption with formation of epithelial cysts (arrow). (D & E) Positive control group on the 5th DPI, severe lymphoid depletion with atrophy and marked necrosis characterized by presence of small sized pyknotic lymphocytes in the germinal center (star) and widened interfollicular spaces with infiltration of inflammatory cells (arrowhead). (F, G) Positive control group on the 7th DPI, showing marked follicular atrophy and lymphoid depletion with lysis of bursal follicles (star) and cystic (C) dilatation in place of lymphoid follicle, also noted extensively widened interfollicular spaces with aggregates of inflammatory cells mainly lymphocytes and macrophages and fibrous connective tissue proliferation (arrowhead). (H) Group A, vaccinated infected, on the 5th DPI severe lesions were noticed represented by vacuolization and lymphocytolysis in the medullary areas (arrow) and follicular atrophy (star) with wide interfollicular space filled with excess fibrous connective tissue and aggregates of mononuclear inflammatory cells (arrowhead). (I) Group A, vaccinated infected, on the 7th DPI, signs of regeneration represented by presence of gland (G) like structure, also noted lymphoid depletion and follicular atrophy (star) with wide interfollicular space filled with aggregates of mononuclear inflammatory cells and fibroblasts (arrowhead).

served, significantly reducing the size and number of lymphoid follicles compared to the negative control group. Additionally, on the 7th DPI, the germinal centers appeared less distinct with prominent signs of atrophy. Interfollicular spaces were widened, and infiltration of inflammatory cells, including lymphocytes and macrophages, was evident throughout the tissue sections. In the vaccinated infected group, histopathological analysis revealed less severe lesions compared to positive control were noticed represented by vacuolization and lymphocytolysis in the medullary areas and follicular atrophy with wide interfollicular space filled with excess fibrous connective tissue and aggregates of mononuclear inflammatory cells. While lymphoid follicles showed signs of hypertrophy similar to the vaccinated group, evidence of lymphoid depletion and follicular atrophy characteristic of IBH infected group was also observed. Interfollicular spaces were widened, and infiltration of inflammatory cells was prominent, reflecting both the protective immune response mounted by vaccination and the pathological consequences of viral infection (Fig. 5).

Kidney

Microscopic examination of kidney tissues from the negative control group revealed typical histological features consistent with a healthy avian kidney. The renal cortex and medulla exhibited well-defined structures, with renal tubules displaying regular epithelial lining and prominent glomeruli. Bowman's capsules appeared intact, enveloping the glomerular tufts, and the renal interstitial showed minimal cellular infil-

tration. Additionally, microscopic examination of kidney tissues from the vaccinated not infected group demonstrated minimal histological changes compared to the negative control group.

Renal tubules maintained regular epithelial morphology, with no evidence of degenerative changes or inflammatory cell infiltration. Glomerular architecture appeared intact, with Bowman's capsules enveloping the glomerular tufts without significant alterations. Histopathological analysis of kidney tissues following IBH infection, infected group (positive control) revealed discernible alterations indicative of viral insult. Renal tubules displayed varying degrees of degenerative changes, including epithelial cell swelling, vacuolization and necrosis. Additionally, massive interstitial inflammation, characterized by lymphocytic infiltration, was observed. Glomerular integrity remained relatively preserved, although focal congestion and hemorrhage were noted in some areas. In vaccinated infected group, the kidney exhibited a mixed histopathological profile indicative of both protective immune response and viral infection. While renal tubules displayed preserved morphology similar to the vaccinated not infected group showed regular epithelial lining of the renal tubules and intact glomerular architecture with no evidence of degenerative changes or inflammatory cell infiltration (Figs. 6 & 7).

Trachea

Microscopic examination of tracheal tissues from the negative control group revealed typical histological features consistent with a healthy

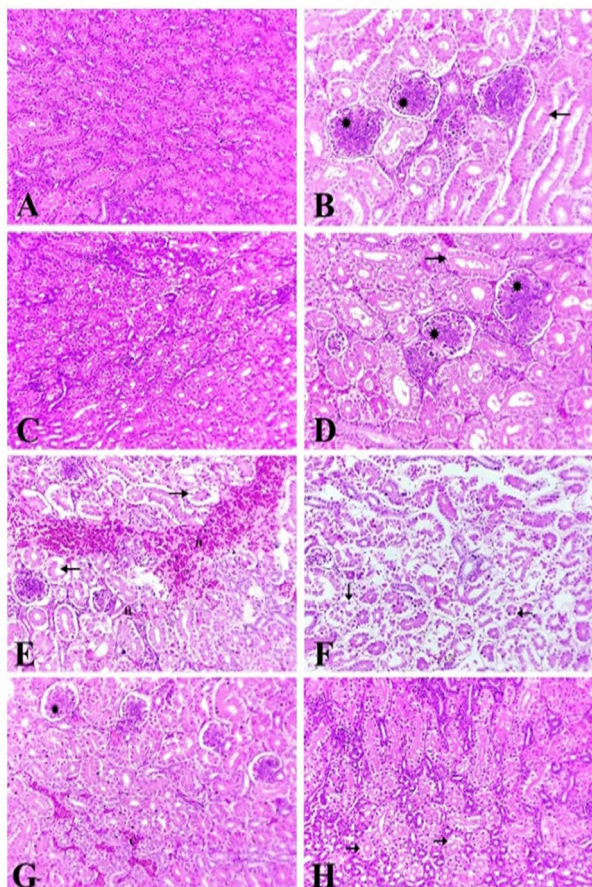


Fig. 6. Histopathological changes of Kidney on the 5th DPI. Control (A, B), vaccinated not infected (C, D), IBH infected (E, F) and vaccinated infected (G, H) groups, H&E, x200. Control group (A, B), showing normal histological appearance of kidney with renal tubules (arrow) displaying regular epithelial lining and prominent glomeruli (star). Vaccinated group (C, D), regular epithelial lining of the renal tubules (arrow) and intact glomerular (star) architecture with no evidence of degenerative changes or inflammatory cell infiltration. IBH infected group (E) distortion of renal parenchyma with hemorrhagic foci (H) in between the degenerated renal tubules (arrow), (F) marked necrosis in the renal tubules represented in pyknotic nuclei and desquamation of the tubular epithelial cells (arrow). Vaccinated infected group (G, H) showing less severe lesion represented in intact glomerular (star) architecture with focal congestion (C) and focal areas of degenerative changes (arrow) in the renal tubules.

avian trachea. The tracheal mucosa exhibited a pseudostratified columnar epithelium with cilia and goblet cells, forming a protective barrier against pathogens. Submucosal glands appeared well-developed, and the cartilaginous rings maintained their structural integrity, supporting the tracheal wall. Tracheal tissues from the vaccinated not infected group demonstrated minimal histological changes compared to the control group. The tracheal epithelium appeared intact, with preserved cilia and goblet cell distribution. Submucosal glands showed no significant alterations, and the cartilaginous rings maintained their structural integrity, similar to negative control group. In IBH infected group (Positive control), the tracheal tissues showed notable alterations indicative of viral infection. The tracheal epithelium exhibited varying degrees of degenerative changes, including loss of cilia and epithelial desquamation. Goblet cell hyperplasia indicated mucous secretion in response to viral insult. Additionally, mild submucosal edema and inflammatory cell infiltration, predominantly lymphocytes, were noted in the lamina propria. The trachea of vaccinated infected group exhibited a mixed histopathological profile indicative of both protective immune response and viral infection (Fig. 8).

Discussion

The current study investigated the clinical, pathological, and mortality outcomes of two distinct avian groups (A and C) infected with a pathogenic strain (FadV-8a), in comparison with two control groups (B and D). Our findings showed that the infected groups A and C exhibited significant clinical signs, and gross pathological changes, but no mortality

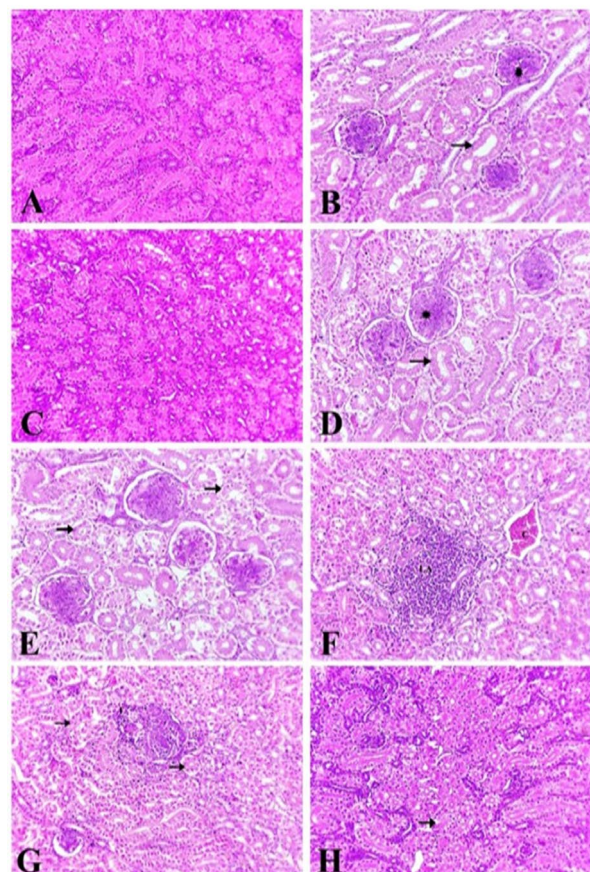


Fig. 7. Histopathological changes of Kidney on the 7th day. Control (A, B), vaccinated not infected (C, D), IBH infected (E, F) and vaccinated infected (G, H) groups, H&E, x200. Control group (A, B), showing normal histological appearance of kidney with renal tubules (arrow) displaying regular epithelial lining and prominent glomeruli (star). Vaccinated group (C, D), regular epithelial lining of the renal tubules (arrow) and intact glomerular (star) architecture with no evidence of degenerative changes or inflammatory cell infiltration. IBH infected group (E) swelling, vacuolization and desquamation of epithelial cells lining renal tubules (arrow), (F) massive interstitial inflammation, characterized by lymphocytic aggregates (LA) in between the degenerated tubules in association with focal congestion (C). Vaccinated infected group (G, H) showing less severe lesion in the form of focal areas of degenerative changes (arrow) and mild interstitial inflammation (I).

were recorded. The results were compared with previous research to contextualize our findings within the broader scientific literature.

Infected birds from groups A and C began showing clinical signs between the 3rd and 9th DPI. The observed symptoms included depression, ruffled feathers, huddling behavior, and in more severe cases profuse diarrhea. These findings align with the clinical manifestations reported in studies by Schachner *et al.* (2018) and Hafez (2011).

The gross pathological examination revealed severe hepatic lesions in infected birds as early as the 5th dpi. These lesions were characterized by a mosaic appearance with clear hemorrhages on the liver. By the 7th dpi, the severity of the hepatic damage had increased, with swollen livers displaying a marble-like pattern ranging from yellow to brown. Hydropericardium was also observed in some cases. These findings are in line with those reported by Nakamura *et al.* (2000) and Radwan *et al.* (2019), who described similar hepatic lesions and hydropericardium in birds infected with IBH virus.

The mosaic and marble-like appearance of the liver, along with petechial and subcapsular hemorrhages, have been well-documented in the literature. For instance, Mariappan *et al.* (2018) observed comparable liver pathologies in birds infected with fowl adenovirus, indicating a common pathogenic mechanism involving hepatic injury and hemorrhaging.

The assessment of virus shedding offers invaluable insights into the mechanisms of viral replication and transmission, thereby enhancing our comprehension of disease progression and facilitating the development of effective control strategies.

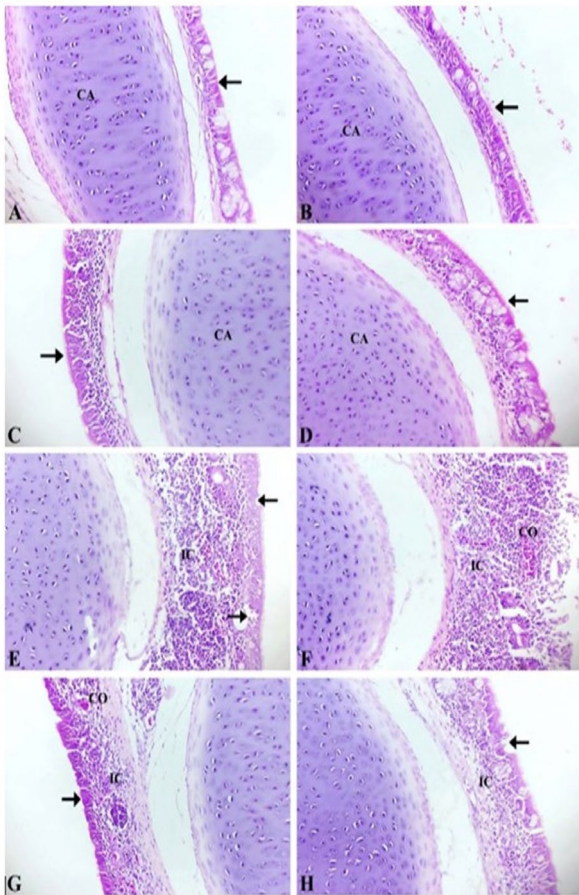


Fig. 8. Histopathological changes of Trachea. control (A: on the 5th day, B: on the 7th day), vaccinated not infected (C: on the 5th day, D: on the 7th day), IBH infected (E: on the 5th day, F: on the 7th day), and vaccinated infected group (G: on the 5th day, H: on the 7th day) groups. The control group showing normal histological appearance of tracheal mucosa exhibited a pseudostratified columnar epithelium with cilia and goblet cells (arrow) and the cartilaginous (CA) rings maintained their structural integrity. Vaccinated group showing intact tracheal epithelium with preserved cilia and goblet cell (arrow) with intact cartilaginous (CA) rings. IBH group, the tracheal epithelium exhibited varying degrees of degenerative changes; loss of cilia and epithelial desquamation (arrow), and congestion (CO) of submucosal blood vessels and inflammatory cell infiltration (IC), predominantly lymphocytes. Vaccinated infected group showing mild degenerative changes in tracheal epithelium (arrow) in association with mild congestion (CO) of submucosal blood vessels and inflammatory cell infiltration (IC).

In this investigation, we explored the shedding dynamics of the Inclusion Body Hepatitis (IBH) virus in broiler chickens subsequent to late infection, with a focus on quantifying viral load using cycle threshold (CT) values and viral titers.

Our findings revealed significant disparities in the dynamics of virus shedding among the experimental groups. Group A, comprising vaccinated and infected birds, demonstrated detectable virus shedding on the 5th, 7th and 9th DPI.

The presence of the virus was evident through positive results and relatively low cycle threshold values, indicative of a higher viral load compared to other groups. Conversely, Groups B and D comprising vaccinated not infected and negative control groups respectively, exhibited no evidence of virus shedding throughout the sampling period. Notably, Group C, serving as the positive control with none vaccinated and infected birds, displayed detectable virus shedding akin to Group A.

The pattern of viral shedding observed in this study is consistent with findings from previous research on IBH and similar viral infections in poultry. Oliver-Ferrando *et al.* (2017) reported that IBH-infected birds exhibited high viral loads shortly after infection, with peak shedding occurred around the 7th DPI. Our findings corroborate this timeline, with the highest titers observed on the 7th dpi and a subsequent decline by 9 dpi.

The blood biochemistry parameters provide crucial insights into the physiological and pathological state of birds infected with Inclusion Body Hepatitis (IBH).

The obtained results revealed significant differences between groups for all parameters ($p < 0.05$). Infected groups (A and C) showed higher lev-

els when compared to negative control and to vaccinated not infected group. The Highest level of Lipase was on the 3rd DPI, for AST was on the 5th and 7th DPI, for total protein and albumin were on the 5th DPI, and for uric acids was on the 5th and 9th DPI. Lipase level generally decreased after infection these trends are consistent with findings from Matos *et al.* (2016), who reported that viral infections often lead to altered lipase activity due to pancreatic damage. The elevation of AST is a hallmark of hepatic injury, as corroborated by Lumeij (2008), who noted that elevated AST activities are indicative of hepatocellular damage in viral hepatitis.

The patterns observed here align with the typical response to IBH infection, reflecting progressive liver damage and the body's attempt to repair and regenerate affected tissues.

The relative stability of albumin levels, despite fluctuations in total protein, suggests a selective impact on liver synthetic functions, as described by Lumeij (2008). Albumin, being a long half-life protein, may not show immediate changes, but its stability amidst total protein fluctuations indicates differential impacts on hepatic protein synthesis pathways. The changes in uric acid levels can be attributed to alterations in renal function and protein metabolism, as viral infections often cause metabolic disturbances, leading to altered excretion patterns.

According to Campbell (2012), elevated uric acid levels post-infection can result from increased protein catabolism and renal stress, which are consistent with the patterns observed in this study.

The observed biochemical changes in this study align with findings from previous research on viral hepatitis in poultry Campbell (2012) reported that IBH infection leads to significant hepatic injury, reflected in elevated AST and altered protein metabolism. Our findings are consistent with this, showed elevated AST and fluctuations in total protein and albumin levels. The changes in lipase activity is consistent with pancreatic dysfunction, as reported by Matos *et al.* (2016) who recorded high levels of blood parameters in infected groups compared to the negative group.

Histopathological alterations in the liver tissues further elucidate the systemic consequences of IBH virus infection. Vacuolar degeneration and cytoplasmic changes in hepatocytes, along with inflammatory cell infiltration and sinusoidal dilatation, reflect the hepatotropic nature of the virus and its ability to induce hepatic injury. The observed portal congestion, bile duct hyperplasia, and perivascular inflammation suggest impairment of liver function and blood flow disruption, potentially contributing to systemic morbidity and mortality. These histopathological results are in agreement with those reported by Wilson *et al.* (2010) and Matos *et al.* (2016) who mentioned that the livers from affected birds exhibited variable and randomly distributed regions with multifocal hepatocellular necrosis and vacuolar degeneration

Interestingly, the vaccinated non-infected group exhibited minimal histological changes in the liver, indicating a protective effect of vaccination against hepatic injury induced by IBH virus infection. However, focal areas of vacuolar degeneration and inflammatory cell infiltration in the vaccinated infected group suggest that while vaccination may reduce the severity of liver pathology, it may not entirely prevent hepatic injury following viral infection.

Histopathological examination of bursa of Fabricius and liver tissues following Inclusion Body Hepatitis (IBH) virus infection in broiler chickens provides crucial insights into the pathogenesis of the disease and the efficacy of vaccination strategies.

The observed histopathological changes in the bursa of Fabricius highlighted the dynamic interplay between viral infection and host immune response. In the IBH infected group, marked lymphoid depletion, follicular atrophy, and infiltration of inflammatory cells signify the destructive effects of viral replication on the lymphoid tissue.

These findings are consistent with previous studies demonstrating the tropism of IBH virus for lymphoid organs and its ability to induce immunosuppression (Naeem *et al.*, 1995; Dutta *et al.*, 2017; Hess, 2020)

Results of the histopathological examination of kidney and tracheal tissues complements the findings from the bursa of Fabricius and liver

and provided a comprehensive understanding of the systemic effects of Inclusion Body Hepatitis (IBH) virus infection and the protective efficacy of vaccination in broiler chickens.

The presence of vacuolization, necrosis, and interstitial inflammation in the IBH infected group signifies the direct cytopathic effects of viral replication on renal epithelial cells and immune-mediated tissue damage. These findings confirm previous studies which demonstrated the nephrotropic nature of IBH virus and its association with renal dysfunction and mortality in affected birds (Wilson *et al.*, 2010).

Conversely, in the vaccinated none infected group, minimal histological changes in the kidney tissues with no evidence of degenerative changes or inflammatory cell infiltration. Although focal areas of degenerative changes and mild interstitial inflammation were observed in the vaccinated infected group indicative of both protective immune response of IB vaccines and IBH viral infection effect on tissue at the same time.

The histopathological alterations observed in the tracheal tissues following IBH infection underscore the respiratory tropism of the virus and its ability to induce epithelial damage and inflammatory responses. The loss of cilia, epithelial desquamation, and goblet cell hyperplasia in the IBH infected group reflect the destructive effects of viral replication on the tracheal epithelium and the host's attempt to clear viral particles through mucous secretion and immune cell recruitment. These findings are consistent with clinical observations of respiratory distress and airway obstruction in IBH-infected birds by Saifuddin and Wilks (1991).

In contrast, the minimal histological changes observed in the tracheal tissues of the vaccinated not infected group suggest a protective effect of vaccination. While focal areas of degenerative changes and goblet cell hyperplasia were noted in the vaccinated infected group, overall tracheal morphology remained relatively preserved, indicating both protective immune response of IB vaccines and IBH viral infection effect on tissue at the same time.

Conclusion

The significant changes in lipase, AST, total protein, albumin, and uric acid levels reflect hepatic and pancreatic injury, altered metabolism, and potential renal stress. Also, histopathological examination contributes to a better understanding of the disease pathology and enhance our understanding of the pathogenesis of IBH virus infection and its interaction towards vaccines in broiler chickens. By elucidating the systemic consequences of viral replication, this study contributes to the development of targeted interventions to minimize disease transmission and improve poultry health and welfare.

Acknowledgments

The authors would like to thank Dr. Mohamed Monir Radwan and Dr. Mahmoud Samir (Animal Health Research Institute, Agriculture Research Center, Egypt) for providing the activated FAdv-8a strain.

Conflict of interest

The authors declare that they have no conflict of interest

References

Adel, A., Mohamed, A.A.E., Samir, M., Hagag, N.M., Erfan, A., Said, M., Hassan, W.M., El Zowalaty, M.E., Shahien, M.A., 2021. Epidemiological and molecular analysis of circulating fowl adenoviruses and emerging of serotypes 1, 3, and 8b in Egypt. *Heliyon* 12, e08366. <https://doi.org/10.1016/j.heliyon.2021.e08366>

Bancroft, J.D., Gamble, M., 2008. In: *Theory and practice of histological techniques*. Elsevier Health Sciences.

Campbell, T.W., 2012. *Clinical chemistry of birds*. In: *Veterinary Hematology and Clinical Chemistry*, 2nd Edition, published by Wiley-Blackwell. pp. 582-598.

Chen, L., Yin, L., Peng, P., Zhou, Q., Du, Y., Zhang, Y., Xue, C., Cao, Y., 2020. Isolation and characterization of a novel fowl adenovirus serotype 8a strain from China. *Virologica Sinica* 35, 517-527. <https://doi.org/10.1007/s12250-019-00172-7>

De Herdt, P., Timmerman, T., Defoort, P., Lycke, K., Jaspers, R., 2013. Fowl adenovirus infections in Belgian broilers: a ten-year survey. *Vlaams Diergeneeskundig Tijdschrift* 82, 125-132. <https://doi.org/10.21825/vdt.v82i3.16704>

Dutta, B., Deka, P., Gogoi, S.M., Sarmah, M., Bora, M.K., Pathak, D.C., 2017. Pathology of inclusion body hepatitis hydropericardium syndrome (IBH-HPS) in broiler chicken. *International Journal of Chemical Studies* 5, 458-461.

Hafez, H.M., 2011. Avian adenoviruses infections with special attention to inclusion body hepatitis/hydropericardium syndrome and egg drop syndrome. *Pakistan Veterinary Journal* 31, 85-92. <http://dx.doi.org/10.17169/refubium-18486>

Harrach, B., Benkö, M., Both, G.W., Brown, M., Davison, A.J., Echavarría, M., Hess, M., Jones, M.S., Kajon, A.L.H.D., Lehmkühl, H.D., Mautner, V., 2011. Family adenoviridae. Virus taxonomy: Classification and nomenclature of viruses. Ninth report of the international committee on taxonomy of viruses, pp. 95-111.

Henry, N.W., Rosenberger, J.K., Lee, K.P., 1978. A clinical evaluation of chickens inoculated with several avian adenovirus isolants. *Avian Diseases* 22, 46-52. <https://doi.org/10.2307/1589506>

Hess, M., 2013. In: *Aviadenovirus infections. Diseases of poultry*, Thirteenth Ed. John Wiley & Sons, pp. 290-300.

Hess, M., 2020. In: *Aviadenovirus infections. Diseases of poultry*, Fourteenth Ed. John Wiley & Sons, pp.322-325.

Köhler, H., Hromatka-Vasicek, L., 1974. Einschlußkörper-Hepatitis bei Broilern in Österreich. *Wien. Tierärztl. Mschr* 61, 90-95.

Lim, T.H., Lee, H.J., Lee, D.H., Lee, Y.N., Park, J.K., Youn, H.N., Kim, M.S., Youn, H.S., Lee, J.B., Park, S.Y., Choi, I.S., 2011. Identification and Virulence Characterization of Fowl Adenoviruses in the Republic of Korea. *Avian Diseases* 6, 554-560. <https://doi.org/10.1637/9894-973011-DIGEST.1>

Lumeij, J.T., 2008. Avian clinical biochemistry. In: *Clinical biochemistry of domestic animals*, Sixth Ed., pp. 839-872. <https://doi.org/10.1016/B978-0-12-370491-7.00030-1>

Maartens, L.H., Joubert, H.W., Aitchison, H., Venter, E.H., 2014. Inclusion body hepatitis associated with an outbreak of fowl adenovirus type 2 and type 8b in broiler flocks in South Africa. *Journal of the South African Veterinary Association* 85, 1-5. <https://hdl.handle.net/10520/EJC163930>

Marek, A., Günes, A., Schulz, E., Hess, M., 2010. Classification of fowl adenoviruses by use of phylogenetic analysis and high-resolution melting-curve analysis of the hexon L1 gene region. *Journal of Virological Methods* 170, 147-154. <https://doi.org/10.1016/j.jviro.2010.09.019>

Mariappan, A.K., Munusamy, P., Latheef, S.K., Singh, S.D., Dhama, K., 2018. Hepato nephropathology associated with inclusion body hepatitis complicated with citrinin mycotoxicosis in a broiler farm. *Veterinary world* 11, p.112. <https://doi.org/10.14202%2Fvetworld.2018.112-117>

Matos, M., Graf, B., Liebhart, D., Schwendenwein, I., Hess, M., 2016. Selected clinical chemistry analytes correlate with the pathogenesis of inclusion body hepatitis experimentally induced by fowl aviadenoviruses. *Avian Pathology* 45, 520-529. <https://doi.org/10.1080/03079457.2016.1168513>

Naeem, K., Niazi, T., Malik, S.A., Cheema, A.H., 1995. Immunosuppressive potential and pathogenicity of an avian adenovirus isolate involved in hydropericardium syndrome in broilers. *Avian Diseases* 39, 723-728. <https://doi.org/10.2307/1592408>

Nakamura, K., Mase, M., Yamaguchi, S., Yuasa, N., 2000. Induction of hydropericardium in one-day-old specific-pathogen-free chicks by adenoviruses from inclusion body hepatitis. *Avian Diseases* 44, 192-196. <https://doi.org/10.2307/1592524>

Ojckic, D., Krell, P.J., Tuboly, T., Nagy, É., 2008. Characterization of fowl adenoviruses isolated in Ontario and Quebec, Canada. *Canadian Journal of Veterinary Research* 72, 236.

Oliver-Ferrando, S., Dolz, R., Calderón, C., Valle, R., Rivas, R., Pérez, M., Biarnés, M., Blanco, A., Bertran, K., Ramis, A., Busquets, N., 2017. Epidemiological and pathological investigation of fowl aviadenovirus serotypes 8b and 11 isolated from chickens with inclusion body hepatitis in Spain (2011-2013). *Avian pathology* 46, 157-165. <https://doi.org/10.1080/03079457.2016.1232477>

Radwan, M.M., El-Deeb, A.H., Mousa, M.R., El-Sanousi, A.A., Shalaby, M.A., 2019. First report of fowl adenovirus 8a from commercial broiler chickens in Egypt: molecular characterization and pathogenicity. *Poultry Science* 98, 97-104. <https://doi.org/10.3382/ps/pey314>

Saifuddin, M., Wilks, C.R., 1991. Pathogenesis of an acute viral hepatitis: inclusion body hepatitis in the chicken. *Archives of Virology* 116, 33-43. <https://doi.org/10.1007/BF01319229>

Sandhu, B.S., Singh, B., Brar, R.S., 1998. Haematological and biochemical studies in broiler chicks fed ochratoxin and inoculated with inclusion body hepatitis virus, singly and in concurrence. *Veterinary Research Communications* 22, 335-346. <https://doi.org/10.1023/A:1006177222023>

Schachner, A., Matos, M., Graf, B., Hess, M., 2018. Fowl adenovirus-induced diseases and strategies for their control—a review on the current global situation. *Avian Pathology* 47, 111-126. <https://doi.org/10.1080/03079457.2017.1385724>

Steer, P.A., O'Rourke, D., Ghorashi, S.A., Noormohammadi, A.H., 2011. Application of high-resolution melting curve analysis for typing of fowl adenoviruses in field cases of inclusion body hepatitis. *Australian Veterinary Journal* 89, 184-192. <https://doi.org/10.1111/j.1751-0813.2011.00695.x>

Tanimura, N., Tsukamoto, K., Nakamura, K., Narita, M., Maeda, M., 1995. Association between pathogenicity of infectious bursal disease virus and viral antigen distribution detected by immunohistochemistry. *Avian Diseases* 39, 9-20. <https://doi.org/10.2307/1591976>

Wilson, F.D., Wills, R.W., Senties-Cue, C.G., Maslin, W.R., Stayer, P.A., Magee, D.L., 2010. High incidence of glomerulonephritis associated with inclusion body hepatitis in broiler chickens: routine histopathology and histomorphometric studies. *Avian Diseases* 54, 975-980.